189
1/15/79

Sh. 2106

DECEMBER 1978 PPPL-1493
UC-20f

MONTE CARLO SIMULATION OF ION TRAJECTORIES IN THE MODIFIED PDX THERMAL CHARGE EXCHANGE ANALYZER

BY

R. KAITA, S. L. DAVIS, S. S. MEDLEY

PLASMA PHYSICS LABORATORY

PRINCETON UNIVERSITY
PRINCETON, NEW JERSEY

This work was supported by the U. S. Department of Energy Contract No. EY-76-C-02-3073. Reproduction, translation, publication, use and disposal, in whole or in part, by or for the United States Government is permitted.

MONTE CARLO SIMULATION OF ION TRAJECTORIES IN THE MODIFIED PDX THERMAL CHARGE EXCHANGE ANALYZER

by

R. Kaita, S. L. Davis, and S. S. Medley
Plasma Physics Laboratory, Princeton University
Princeton, N. J. 08540

ABSTRACT

An improved design for the present PDX thermal charge exchange analyzer (MACE) has been proposed by one of the authors, in which the five cylindrical electrostatic plates for mass separation are replaced by a single flat, electrostatic deflection plate. An existing Monte Carlo code that simulated the passage of ions through the MACE analyzer was modified to examine the feasibility of this change. The resulting calculations were used to optimize detector positions and collimation requirements. The first analyzer to be placed on PDX will be of the old design, similar to the present PLT analyzer. However, if the design reported here is successful on the test stand, the future PDX analyzers will all be of the new, single electrostatic plate variety. A further advantage will be the ability to install as many as ten detectors instead of the current five, thus providing twice as many energy channels for each shot. Also, both mass species (H, D) can be measured concurrently, if desired.

I. INTRODUCTION

The present PLT and PDX charge exchange analyzer consists of a stripping cell, a 120° deflection magnet for energy resolution, and a set of five cylindrical electrostatic deflection plates for mass separation.[1] The magnet is used to focus only particles of E and E/2 onto the entrance apertures of the electrostatic plates, so by setting the voltage on a given plate, only one ion species will follow a trajectory of the proper curvature to pass through the system and be detected (Fig. 1a.).

Since it is only necessary to separate hydrogen and deuterium ions, however, the geometry can be greatly simplified by installing a flat, electrostatic deflection plate in place of the cylindrical plates (Fig. 1b.). The electric field is now normal to the plane of the diagram, and charge separation is effected because particles of E and E/2 are deflected by different amounts in this vertical direction after traversing the same horizontal distance across the plate.

A Monte Carlo code (MACE.FOR)[2] was originally written to estimate the absolute efficiency of the existing analyzer. It simulates a source of particles having a spread in both energy and angle as specified by the user. The trajectory of each particle is calculated in accordance with the electromagnetic fields it passes through in the various parts of the analyzer. If the coordinates of the particle exceed those for an aperture, pole face, or plate it encounters, the particle is recorded as "lost" at that location and the trajectory for a new particle is initiated at the particle source.

II. SIMULATION CODE FOR THE MODIFIED MACE ANALYZER

The new simulation code (MACSYM.FOR) is the same as MACE.FOR, except for slight modifications in the input structure, until the calculations for the passage across the electrostatic deflection plate are done. Referring to Fig. 2, a given particle enters the analyzing magnet and is deflected away from the l-axis according to $mv^2/r=qvB$. That is, if ds is the element of path length along the particle trajectory, the l and y coordinates of the particle are generated according to:

$$l_i = l_{i-1} + \left(\frac{dl}{ds}\right)_i ds \quad , \tag{1}$$

$$y_i = y_{i-1} + \left(\frac{dy}{ds}\right)_i ds \quad , \tag{2}$$

$$\left(\frac{dl}{ds}\right)_i = \left(\frac{dl}{ds}\right)_{i-1} - \left(\frac{dy}{ds}\right)_i \cdot ds \cdot \left(\frac{1}{R_{mag}}\right) \quad , \tag{3}$$

$$\left(\frac{dy}{ds}\right)_i = \left(\frac{dy}{ds}\right)_{i-1} + \left(\frac{dl}{ds}\right)_i \cdot ds \cdot \left(\frac{1}{R_{mag}}\right) \quad . \tag{4}$$

This is because the deflection is proportional to B, and B in turn is inversely proportional to R_{mag}. If l is less than

$$l = 1.73\,y - 6.9 \quad , \tag{5}$$

the equation for the exit edge of the magnet, the field is "turned off" ($B=1/R_{mag}=0$ such that (dl/ds) and (dy/ds) are constant).

Beyond the magnet edge, the trajectory is unaffected and linear until l is less than

$$l = 1.73\,y - 9 \quad , \tag{6}$$

the equation for the leading edge of the flat electrostatic deflection plate. The motion in the l,y plane is still governed by constant dl/ds and dy/ds, but now, a force normal to this plane is introduced. It is given by:

$$m \frac{d^2x}{dt^2} = q\varepsilon = \frac{V}{d} \tag{7}$$

where d is the gap between the plate and ground potential, and V is the plate voltage. From

$$E = \frac{1}{2} mv^2 = \frac{1}{2} m\left(\frac{ds}{dt}\right)^2 \quad , \tag{8}$$

or

$$(dt)^2 = \frac{m}{2E} (ds)^2 \quad , \tag{9}$$

we get

$$m \frac{d^2x}{\left(\frac{m}{2E}\right) (ds)^2} = \frac{V}{d} \tag{10}$$

and hence

$$\frac{d^2x}{ds^2} = \frac{V}{2Ed} \quad . \tag{11}$$

The x-coordinate (normal to the plane of Fig. 2) now changes by

$$x_i = x_{i-1} + \left(\frac{dx}{ds}\right)_i ds \quad , \tag{12}$$

$$\left(\frac{dx}{ds}\right)_i = \left(\frac{dx}{ds}\right)_{i-1} + \left(\frac{d^2x}{ds^2}\right) ds \tag{13}$$

so that

$$\left(\frac{dx}{ds}\right)_i = \left(\frac{dx}{ds}\right)_{i-1} + \left(\frac{V}{2Ed}\right) ds \quad . \tag{14}$$

The calculation continues until either x is larger than d, in which case the particle is recorded as having hit the plate, or l is less than

$$l = .74\ y = 9.4 \quad , \qquad (15)$$

the equation for the exit edge of the electrostatic plate. Any particle that gets this far is considered detected.

III. RESULTS

Two mass separation cases were tried. The first used particles having energy spreads of $0.85 < E < 1.15$ and $.425 < E < .575$. This simulated the situation where hydrogen ions of energy spread $0.85 < E < 1.15$ were to be detected. Figure 3 shows a plot of vertical (x-direction) deflection (cm) as a function of distance (cm) along the detector plane. A primary reason for doing a computer simulation was to study the effectiveness of the new mass separation scheme in resolving the hydrogen ions from the deuterium ions. Therefore, although the less energetic deuterium ions would be lost on the electrostatic plate and not detected in this first case (the distance between the plate and ground being 4 cm), the distribution of these ions was still plotted on Fig. 3 to make sure that it did not overlap with the distribution for the hydrogen ions, and hence give spurious contributions to our measurements. What we actually find is that the two ion species are clearly separated, and it appears that a 0.8 cm wide detector centered at 2.5 cm should detect most of the hydrogens. It is important to note that 2.5 is the mean total vertical deflection, so that if particles are assumed, for example, to enter the electrostatic plate region 1 cm above ground, the detector should be placed at a height of 3.5 cm.

Figure 4 shows the dispersion of particles along the plane of the detector as a function of particle energy along this plane. What this suggests is that for an energy resolution of ± 0.1 at E = 1, a vertical slit of about 1.3 cm in width should be sufficient. For ± 0.1 at E = 5, however, a slit of width 0.8 cm is needed.

The second case used particles having energy spreads of $1.70 < E < 2.30$ and $0.85 < E < 1.15$ (or equivalently, a case where the plate voltage is halved). Here, deuterium ions of energy $0.85 < E < 1.15$ were to be detected. From Fig. 5, it can again be recommended that we use a 0.8 cm wide detector centered at 2.5 cm. According to Fig. 6, we also require a vertical slit of about 1.6 cm in width for an energy resolution of ± 0.1 at E = 1, and a slit of about 0.5 cm in width for comparable resolution at E = 5. This tendency of needing a decreasing slit width with increasing energy, incidentally, agrees with experience from the existing five-channel MACE analyzer. In the two cases discussed above, the plate potential was fixed at 1 kV and the angular spread of the incident particles was $\Delta\phi = 0.03$ radians (1.7°), or more than enough to flood the entrance of the MACE system.

These calculations were repeated using entrance and exit fringe fields for the MACE magnet of the form:

$$B_{fringe}(u) = 1/2\ (1 - \tanh(u)) \qquad (16)$$

where u is the distance between the ion and magnet edge. A plot of vertical deflection of particles having energy spreads of $1.70 < E < 2.30$ and $0.85 < E < 1.15$ as a function of distance along the detector plane if these fringe fields are imposed is shown in Fig. 7. The relationship between particle energy and distance traveled in the electrostatic field is not linear for a fixed vertical deflection, and because the exit edge is straight, we continue to see a slight curvature in the mean location of the particles across the detector plane. This can be easily corrected when the plate is actually built, but even in the design studied here, the ion species, though shifted slightly in absolute position, are still clearly separated. Furthermore, the dispersion curve shown in Fig. 8 indicates that the slit requirements for an energy resolution of ± 0.1 are essentially the same.

IV. CONCLUSIONS

The Monte Carlo simulation studies indicate that the modified MACE analyzer should have sufficient mass separating capability. Furthermore, according to the second case, the design would allow the detection of both ion species simultaneously if a 0.5 cm wide detector were centered at 1.25 cm and a 0.8 cm detector were centered at 2.5 cm. Although this configuration is possible with the channeltrons now installed, using channel plates instead would be both more convenient and economical. The present MACE analyzer, in contrast, could only be adjusted for one type of ion at a time. Calculations that include the effects of a realistic drift distance between the electrostatic plate exit and the detector face and the presence detector apertures are planned to make the simulation more complete.

ACKNOWLEDGMENTS

The authors would like to thank R. J. Goldston for many helpful discussions. This work was supported by the United States Department of Energy contract number EY-76-C-02-3073.

REFERENCES

1. S.L. Davis, S.S. Medley, and M. Brusati, "The Charge Exchange Analyzer for the Mass Resolved Ion Temperature Measurements on PLT," PPPL-1478 (1978).

2. S. L. Davis and R. J. Goldston, MACE.FOR (unpublished).

FIGURE CAPTIONS

Figure 1a. Field geometry of present PLT and PDX charge exchange analyzer. (786362)

Figure 1b. Proposed new design for PDX charge exchange analyzer. (786362)

Figure 2. New PDX charge exchange analyzer showing coordinate system used in ion trajectory calculations. (786361)

Figure 3. Scatter plot for particles of energy E/2 and E on detector plane. (786364)

Figure 4. Dispersion of particles of energy E/2 and E along detector plane as function of particle energy. (786360)

Figure 5. Scatter plot for particles of energy 2E and E on detector plane. (786365)

Figure 6. Dispersion of particles of energy 2E and E along detector plane as function of particle energy. (786363)

Figure 7. Scatter plot for particles of energy 2E and E on detector plane with magnet fringe fields included. (786396)

Figure 8. Dispersion of particles of energy 2E and E along detector plane as a function of particle energy with magnet fringe fields included. (786395)

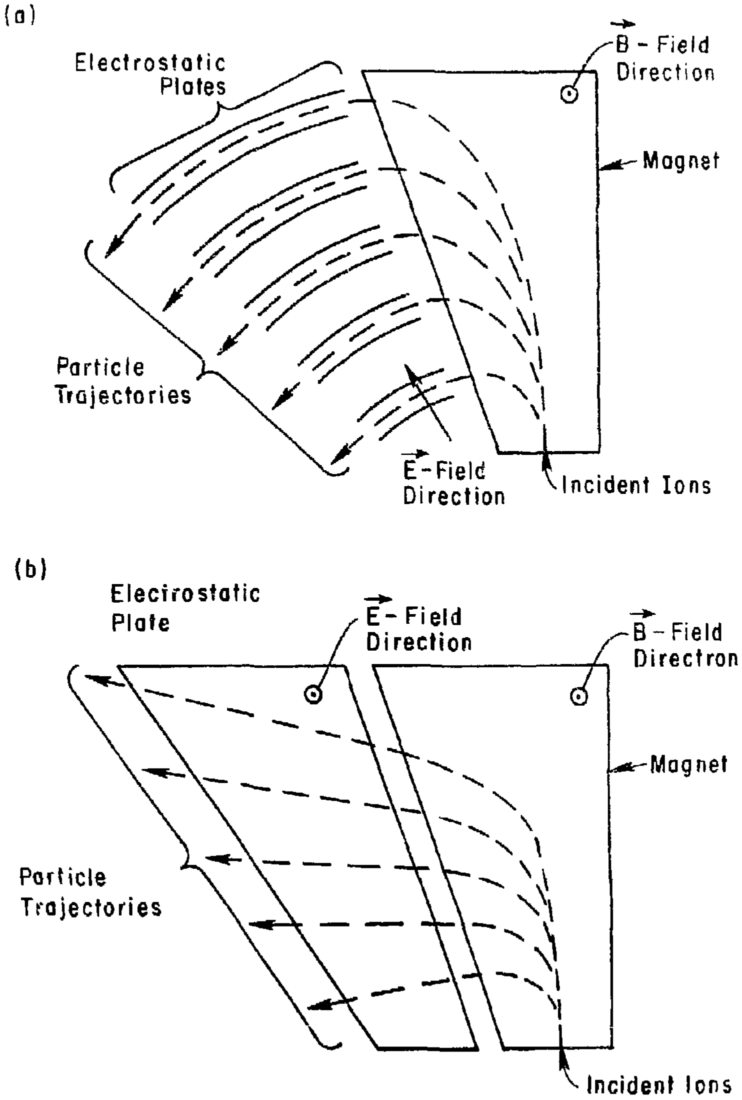
(a)
Electrostatic Plates
$\vec{B}$ - Field Direction
Magnet
Particle Trajectories
$\vec{E}$-Field Direction
Incident Ions
(b)
Electrostatic Plate
$\vec{E}$- Field Direction
$\vec{B}$ - Field Directron
Magnet
Particle Trajectories
Incident Ions

Fig. 1. 786362

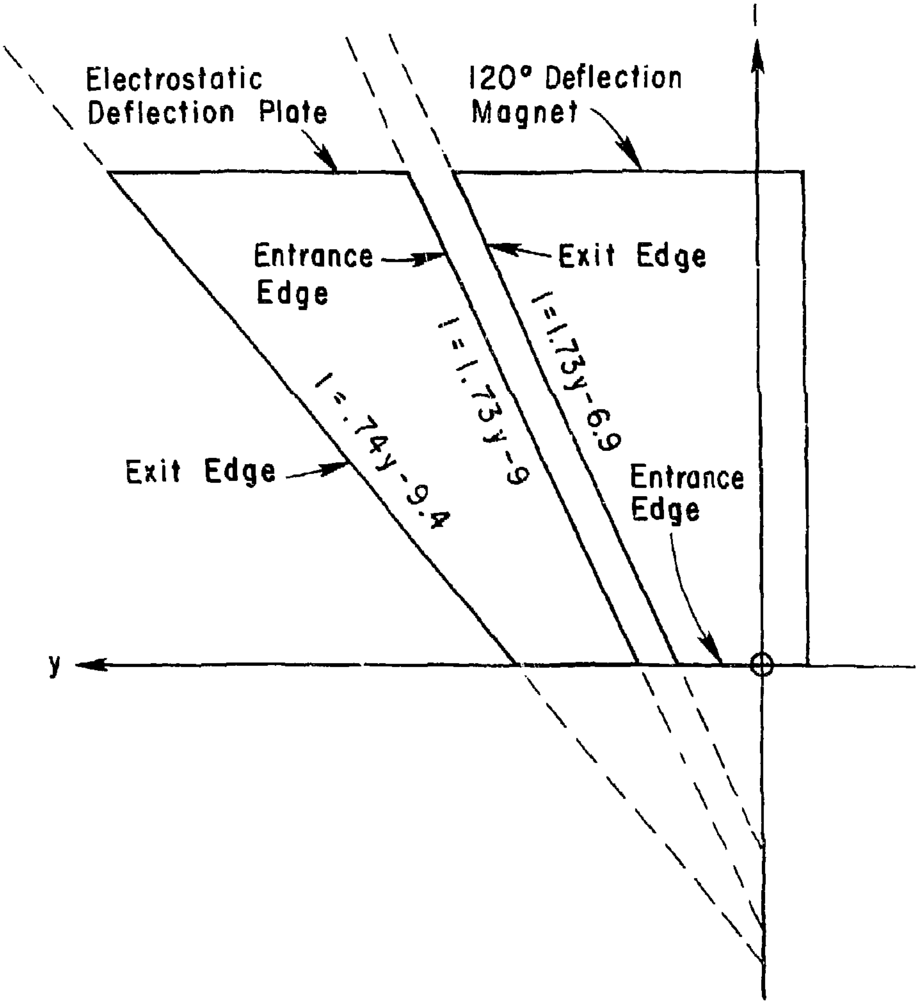
Electrostatic Deflection Plate
120° Deflection Magnet
Entrance Edge
Exit Edge
l = .74y - 9.4
l = 1.73y - 9
l = 1.73y - 6.9
Exit Edge
Entrance Edge
y
l

Fig. 2. 786361

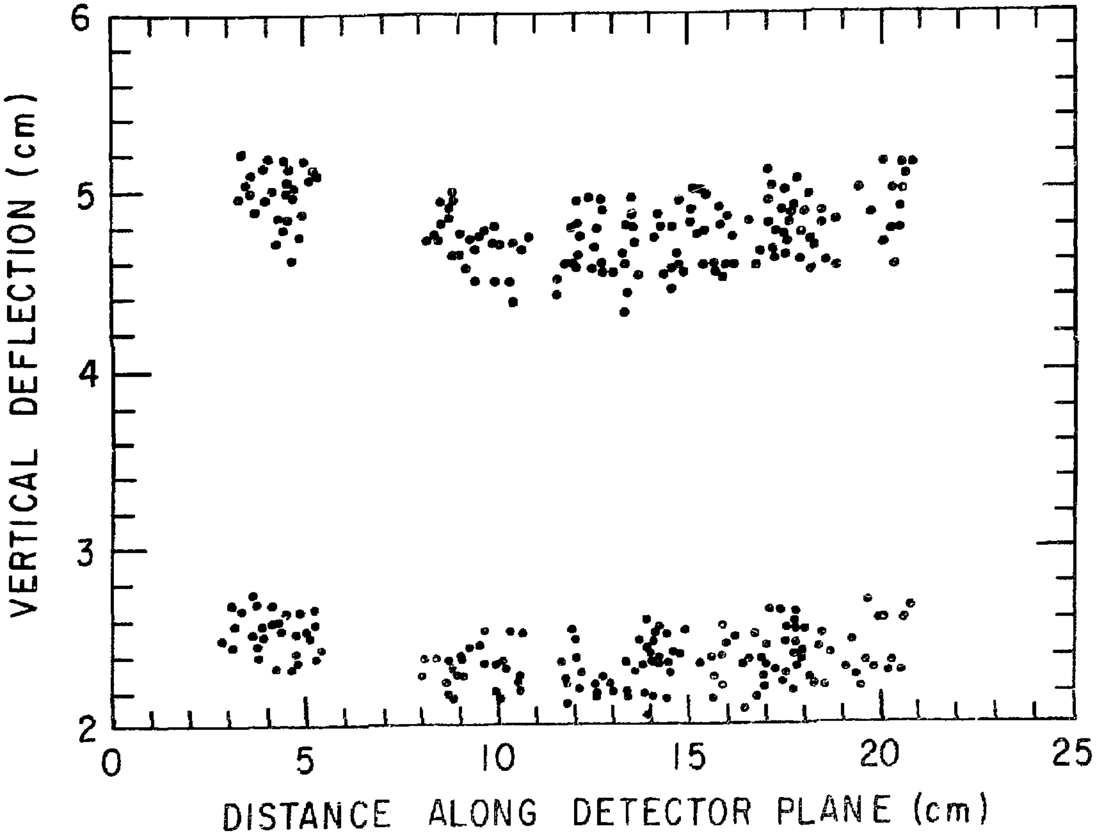
6
5
4
3
2
0
5
10
15
20
25
VERTICAL DEFLECTION (cm)
DISTANCE ALONG DETECTOR PLANE (cm)

Fig. 3. 786364

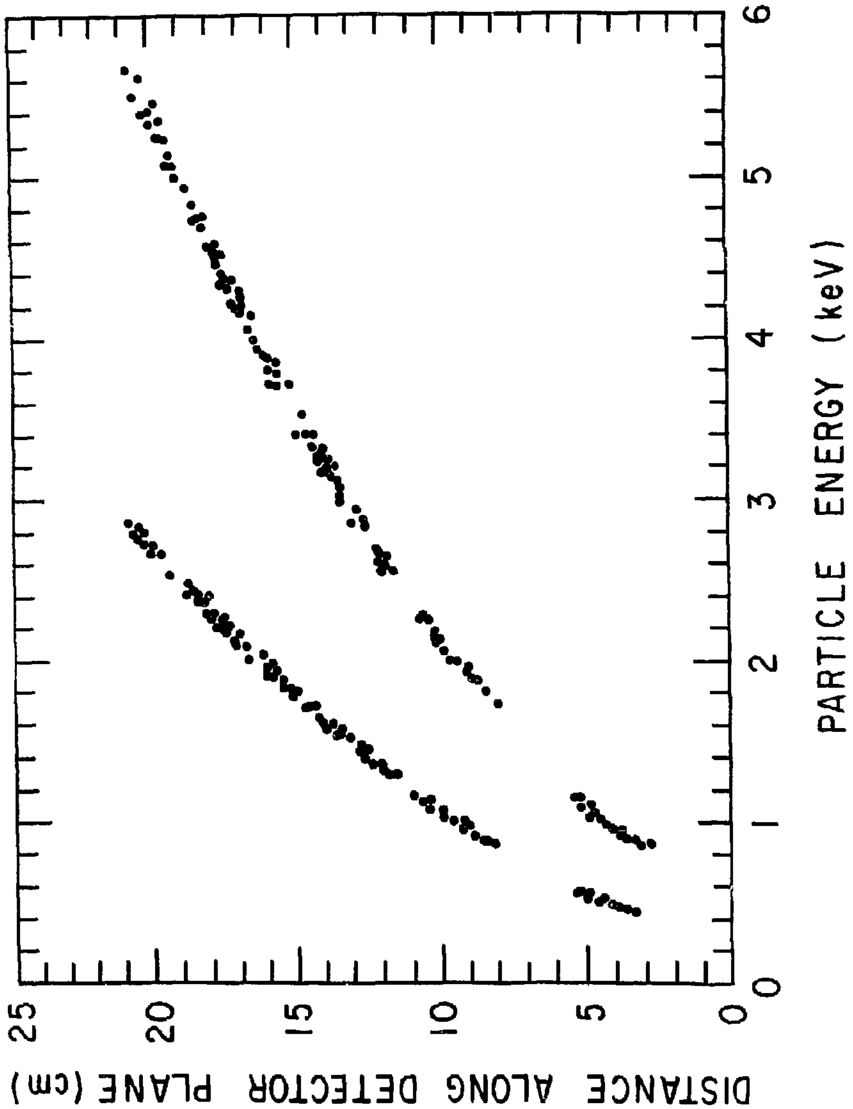
DISTANCE ALONG DETECTOR PLANE (cm)
0
5
10
15
20
25
PARTICLE ENERGY (keV)
0
1
2
3
4
5
6

Fig. 4. 786360

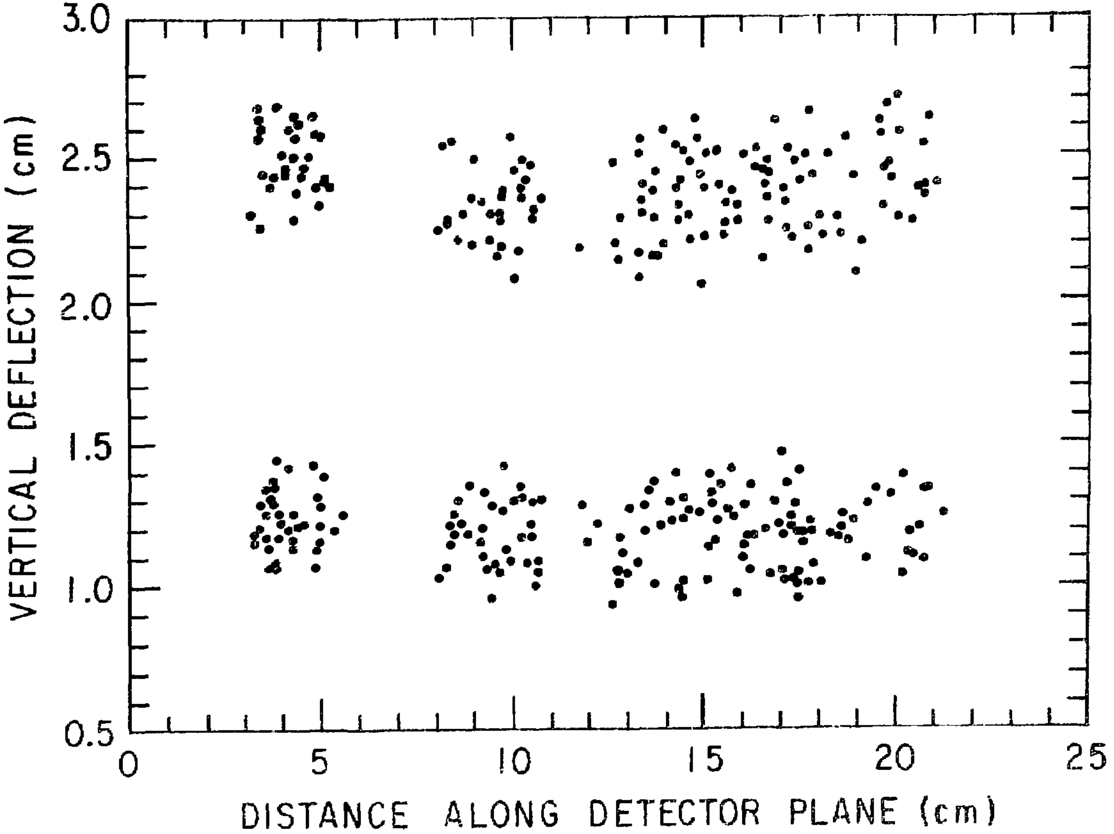
3.0
2.5
2.0
1.5
1.0
0.5
VERTICAL DEFLECTION (cm)
0
5
10
15
20
25
DISTANCE ALONG DETECTOR PLANE (cm)

Fig. 5. 786365

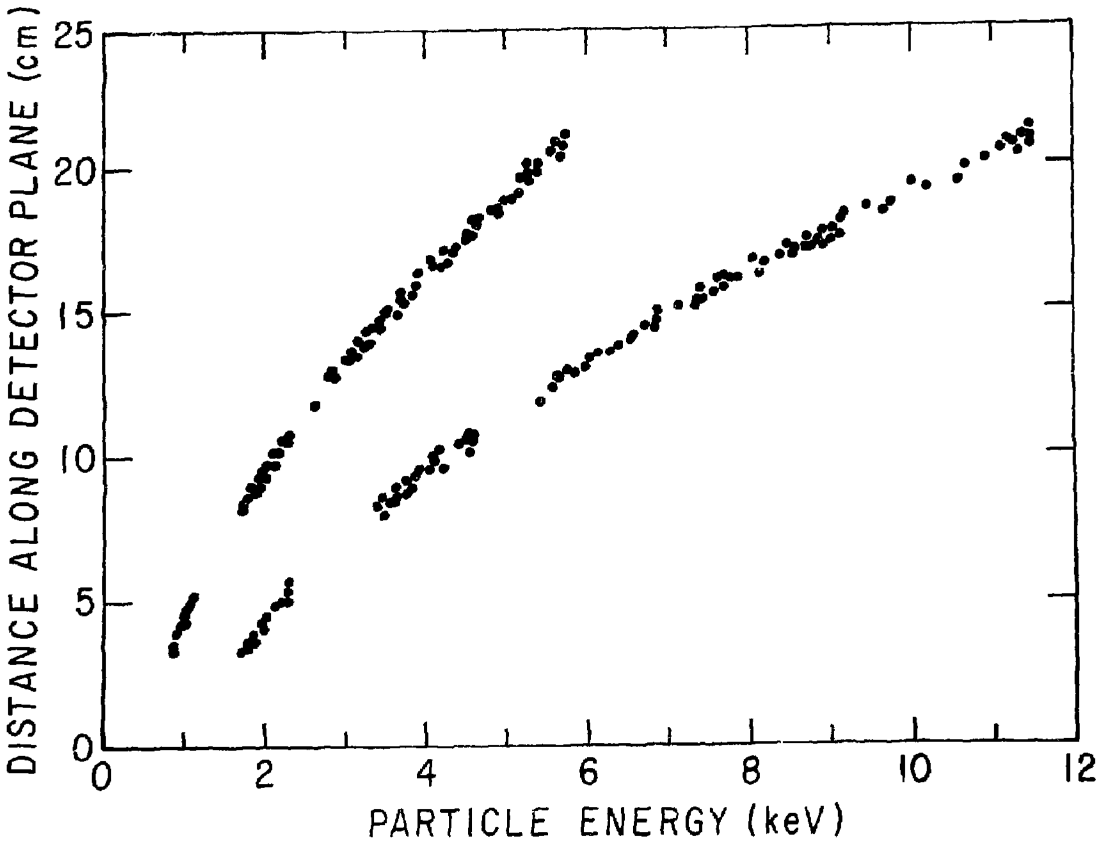
DISTANCE ALONG DETECTOR PLANE (cm)
0
5
10
15
20
25
0
2
4
6
8
10
12
PARTICLE ENERGY (keV)

Fig. 6. 786363

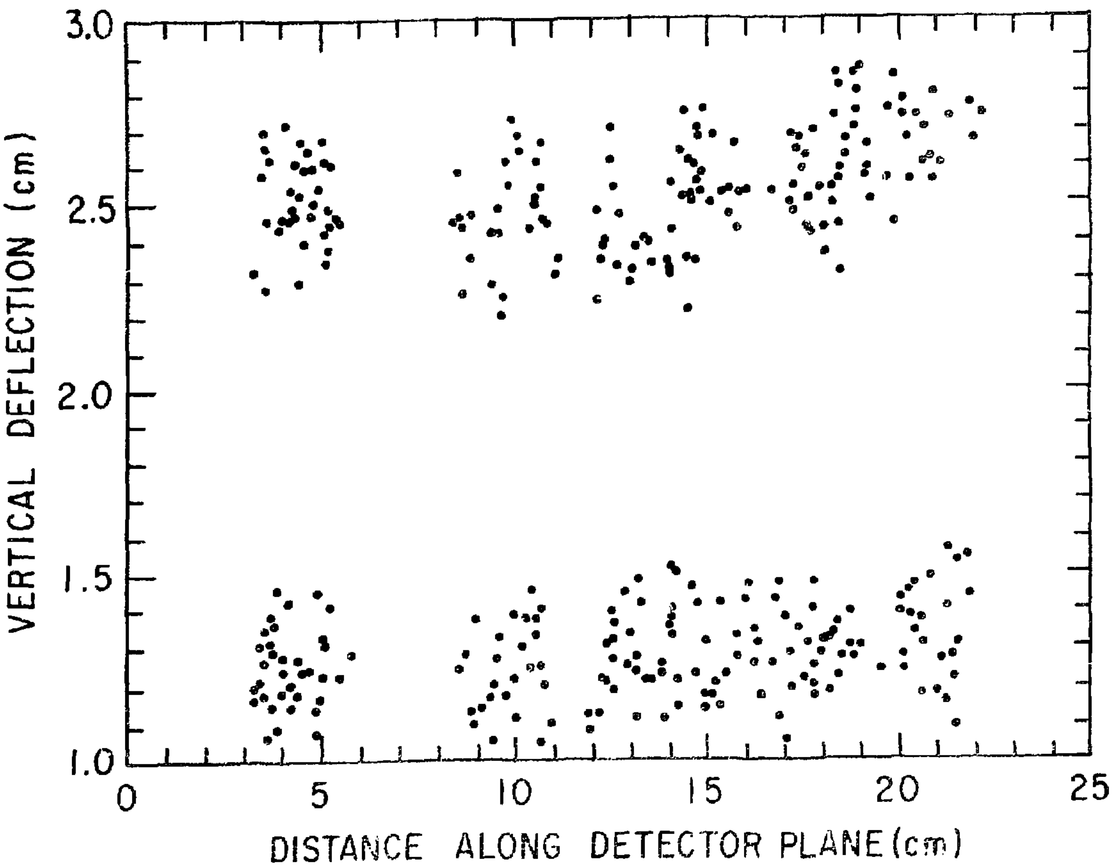
VERTICAL DEFLECTION (cm)
3.0
2.5
2.0
1.5
1.0
0
5
10
15
20
25
DISTANCE ALONG DETECTOR PLANE (cm)

Fig. 7. 786396

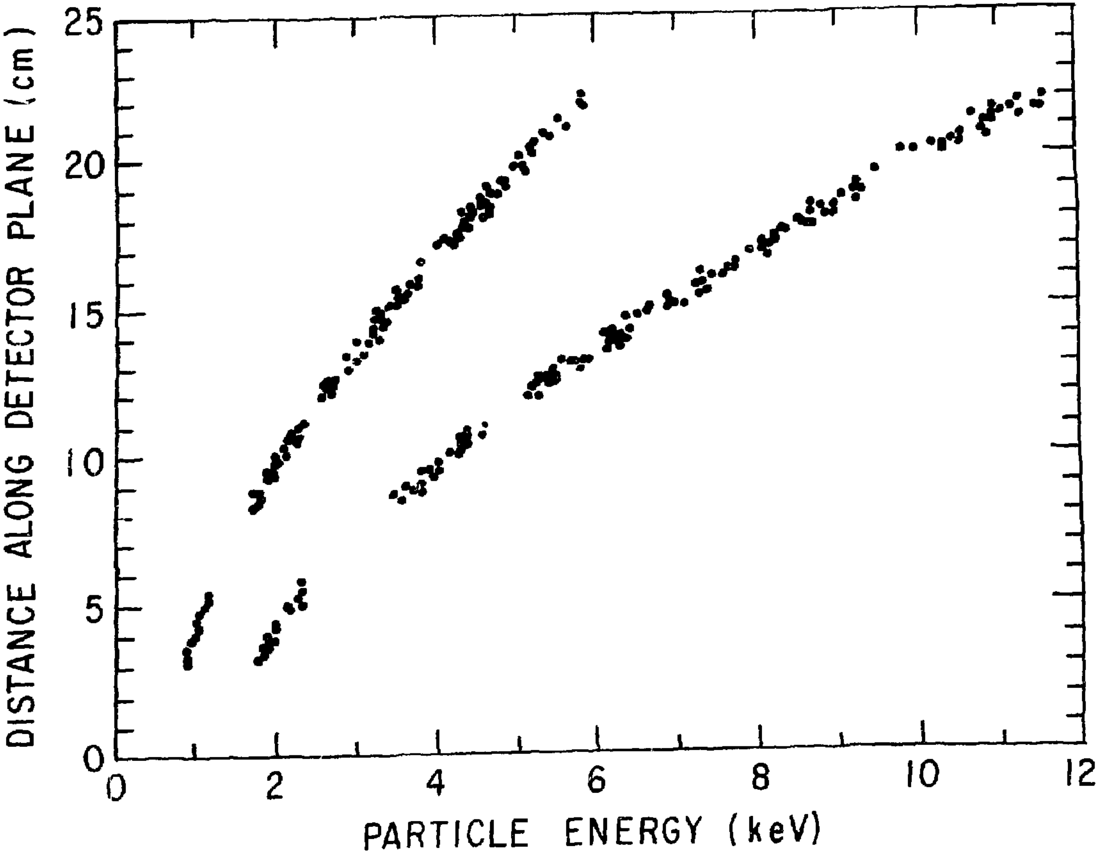
DISTANCE ALONG DETECTOR PLANE (cm)
0
5
10
15
20
25
0
2
4
6
8
10
12
PARTICLE ENERGY (keV)

Fig. 8. 786395

EXTERNAL DISTRIBUTION IN ADDITION TO TIC UC-20

ALL CATEGORIES

- R. Askew, Auburn University, Alabama
- S. T. Wu, Univ. of Alabama
- Geophysical Institute, Univ. of Alaska
- [illegible] Johnston, Sonoma State Univ, California
- H. H. Kuehl, Univ. of S. California
- Institute for Energy Studies, Stanford University
- H. D. Campbell, University of Florida
- N. L. Oleson, University of South Florida
- W. M. Stacey, Georgia Institute of Technology
- Benjamin Ma, Iowa State University
- Magne Kristiansen, Texas Tech. University
- W. L. Wiese, Nat'l Bureau of Standards, Wash., D.C.
- Australian National University, Canberra
- C.N. Watson-Munro, Univ. of Sydney, Australia
- F. Cap, Inst. for Theo. Physics, Austria
- Ecole Royale Militaire, Bruxelles, Belgium
- D. Palumbo, Comm. of Eur. Comm., Belgium
- P.H. Sakanaka, Instituto de Fisica, Campinas, Brazil
- C.R. James, University of Alberta, Canada
- T.W. Johnston, INRS-Energie, Vareenes, Quebec
- H. M. Skarsgard, Univ. of Saskatchewan, Canada
- Librarian, Culham Laboratory, Abingdon, England
- A.M. Dupas Library, C.E.N.-G, Grenoble, France
- Central Res. Inst. for Physics, Hungary
- R. Shingal, Meerut College, India
- M. Naraghi, Atomic Energy Org. of Iran
- Biblioteca, Frascati, Italy
- Biblioteca, Milano, Italy
- G. Rostagni, Univ. Di Padova, Padova, Italy
- Preprint Library, Inst. de Fisica, Pisa, Italy
- Library, Plasma Physics Lab., Gokasho, Uji, Japan
- S. Mori, Japan Atomic Energy Res. Inst., Tokai-Mura
- Research Information Center, Nagoya Univ., Japan
- S. Shioda, Tokyo Inst. of Tech., Japan
- Inst. of Space & Aero. Sci., Univ. of Tokyo
- T. Uchida, Univ. of Tokyo, Japan
- H. Yamato, Toshiba R. & D. Center, Japan
- M. Yoshikawa, JAERI, Tokai Res. Est., Japan
- N. Yajima, Kyushu Univ., Japan
- R. [illegible]stand, Univ. Nacional Auto-noma de Mexico
- [illegible], Univ. of Waikato, New Zealand
- [illegible]ss, Saab Univas Norge, Norway
- J. M. Cabral, Univ. de Lisboa, Portugal
- O. Petrus, AL.I. CUZA Univ., Romania
- J. de Villiers, Atomic Energy Bd., South Africa
- A. Maurech, Comisaria De La Energy y Recoursos Minerales, Spain
- Library, Royal Institute of Technology, Sweden
- Cen. de Res. En Phys.Des Plasmas, Switzerland
- Librarian, Fom-Instituut Voor Plasma-Fysica, The Netherlands
- V. E. Golant, A.F. Ioffe Physical-Tech. Inst., USSR
- B.B. Kadomtsev, Kurchatov Inst. of Atomic Energy, USSR
- The Kharkov Physical-Tech. Inst., USSR
- M. S. Rabinovich, Academy of Sci, USSR
- Bibliothek, Stuttgart, West Germany
- R.D. Buhler, Univ. of Stuttgart, West Germany
- Max-Planck-Inst. fur Plasmaphysik, W. Germany
- Nucl. Res. Estab., Julich, West Germany
- K. Schindler, Inst. Fur Theo. Physik, W. Germany

EXPERIMENTAL THEORETICAL

- M. H. Brennan, Flinders Univ. Australia
- H. Barnard, Univ. of British Columbia, Canada
- S. Screenivasan, Univ. of Calgary, Canada
- J. Radet, C.E.N.-B.P., Fontenay-aux-Roses, France
- Prof. Schatzman, Observatoire de Nice, France
- S. C. Sharma, Univ. of Cape Coast, Ghana
- R. N. Aiyer, Laser Section, India
- B. Buti, Physical Res. Lab., India
- L. K. Chavda, S. Gujarat Univ., India
- I.M. Las Das, Banaras Hindu Univ., India
- S. Cuperman, Tel Aviv Univ., Israel
- E. Greenspan, Nuc. Res. Center, Israel
- P. Rosenau, Israel Inst. of Tech., Israel
- Int'l. Center for Theo. Physics, Trieste, Italy
- I. Kawakami, Nihon University, Japan
- T. Nakayama, Ritsumeikan Univ., Japan
- S. Nagao, Tohoku Univ., Japan
- J.I. Sakai, Toyama Univ., Japan
- S. Tjotta, Univ. I Bergen, Norway
- M.A. Hellberg, Univ. of Natal, South Africa
- H. Wilhelmson, Chalmers Univ. of Tech., Sweden
- Astro. Inst., Sonnenborgh Obs., The Netherlands
- N.G. Tsintsadze, Academy of Sci GSSR, USSR
- T. J. Boyd, Univ. College of North Wales
- K. Hubner, Univ. Heidelberg, W.Germany
- H. J. Kaeppeler, Univ. of Stuttgart, West Germany
- K. H. Spatschek, Univ. Essen, West Germany

EXPERIMENTAL ENGINEERING

- B. Grik, Univ. de Quebec, Canada
- P. Lukac, Komenskeho Univ., Czechoslovakia
- G. Horikoshi, Nat'l Lab for High Energy Physics, Tsukuba-Gun, Japan
- V. A. Glukhikh, D.V. Efremov Sci. Res. Instit.of Elect. App., USSR

EXPERIMENTAL

- F. J. Paoloni, Univ. of Wollongong, Australia
- J. Kistemaker, Fom Inst. for Atomic & Molec. Physics, The Netherlands

THEORETICAL

- F. Verheest, Inst. Vor Theo. Mech., Belgium
- J. Teichmann, Univ. of Montreal, Canada
- T. Kahan, Univ. Paris VII, France
- R. K. Chhajlani, India
- S. K. Trehan, Panjab Univ., India
- T. Namikawa, Osaka City Univ., Japan
- H. Narumi, Univ. of Hiroshima, Japan
- Korea Atomic Energy Res. Inst., Korea
- E. T. Karlson, Uppsala Univ., Sweden
- L. Stenflo, Univ. of UMEA, Sweden
- J. R. Saraf, New Univ., United Kingdom